Measurement of the scaling of the dissipation at high Reynolds numbers

G. Zocchi, P. Tabeling, J. Maurer, and H. Willaime
Laboratoire de Physique Statistique, Ecole Normale Superieure, 24 Rue Lhomond, 75005 Paris Cedex, France
(Received 15 April 1994; revised manuscript received 22 July 1994)

We present experimental results from a mechanically driven turbulent flow in helium gas at low temperature. A large range of Reynolds numbers, extending over three decades (up to 5000 for R_λ) is investigated. We perform torque measurements and determine the dissipation locally by two methods, using the third-order structure function and the energy spectrum. Related quantities, such as the Kolmogorov and Taylor scales, and determined. Both methods give consistent measurements for $R_\lambda > 1000$ but differences are observed at lower values. The scaling of the dissipation is determined by using a single power law to fit the whole range of Reynolds numbers; we recover the classical value (exponent equal to 3) when dissipation is calculated by using a third-order structure function, while a significantly lower value is obtained when a spectral method is used. The question of the viscosity dependence of the dissipation is thus left open. Several issues, such as the anisotropy, homogeneity of the flow, and Taylor hypothesis are discussed.

PACS number(s): 47.27.−i

I. INTRODUCTION

During more than forty years, outstanding experimental studies have been carried out in the field of turbulence [1]; despite this effort, there still remain several basic assumptions which seem worthwhile to compare more precisely with experiment. This is the case for the law of constancy of the dissipation, which states that the energy dissipation rate remains finite as the viscosity tends to zero, or equivalently that the dissipation scales as the cube of the velocity of the energy containing eddies. This "inviscid estimate" of the dissipation is considered as a cornerstone of turbulence theory [2] because its validity is a condition for the existence of an inertial range; if it is violated, then viscosity invades all scales of the flow and it is no longer possible to define a range where energy is transferred, without loss, from large to small scales [3]. Up until now, no observation has contradicted this assumption, but on the other hand, there is no compelling experimental evidence for it. The fact that the drag coefficient is roughly independent of the Reynolds number is generally understood as an indirect proof of this law. Similar considerations apply for the friction factor in duct flows. The law of dissipation has been checked more directly some time ago, in a range of Taylor scale Reynolds numbers extending from 50 to 500 [4]. In view of its importance, one may wish to investigate the validity of this assumption at larger values of the Reynolds number, where an asymptotic regime is likely to be reached.

We address this question with the present experiment, which is designed to reach very high Reynolds numbers and also span a wide range. Following the work on convection by Heslot, Castaing, and Libchaber [5], we achieve this using helium gas at low temperature. By changing the density (from the critical point region, $T \sim 5$ K, $p \sim 2$ atm, down to pressures of a few mbars at ~ 5 K) we can vary the kinematic viscosity ν by three orders of magnitude, and cover the range $10^4 < \mathrm{Re} < 10^7$, or in terms of the Reynolds number calculated on the Taylor scale: $100 < R_\lambda < 5000$ (see Sec. II for the definition of Re and Sec. IV for that of R_λ). The objective of this paper is thus to present measurements of the dissipation and related quantities such as the Taylor and Kolmogorov scales. The dissipation is determined locally by two different methods: the first one uses the third-order structure function, and relies on the von-Karman–Howarth relation, while the second one uses the energy spectrum. We also present measurements of the torque exerted on one of the disks.

II. EXPERIMENTAL SETUP

Figure 1 shows a schematic of the experimental system that we have used in the present study (in some cases, we

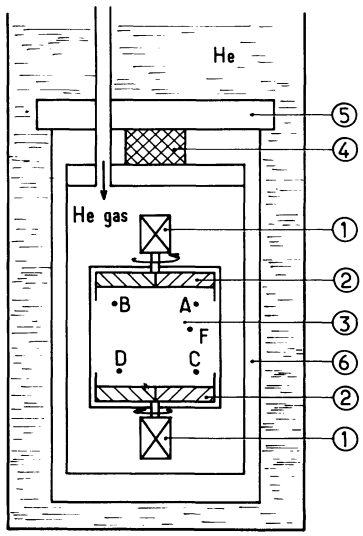

FIG. 1. Sketch of the experimental system. 1: dc motors, 2: blades fixed on the rotating disks, 3: working fluid, 4: thermal link, 5: copper plate, 6: vacuum; Positions of probes are indicated by letters A–D and F.

 ©1994 The American Physical Society

shall refer to a smaller device, described in Ref. [6]). The flow is mechanically driven by two counterrotating disks of diameter 20 cm enclosed in a cylindrical envelope. The disks have the profile of a U (to counterbalance the centrifugal force at the edge) and each of them is equipped with six radial straight blades (of height 2 cm) in order to increase the entrainment [7]. They are driven by dc motors at frequencies between 1–10 Hz. Without blades it was found difficult to obtain large average velocities a few centimeters away from the disks, this condition being important from the point of view of the measurement, because it ensures that the anemometer is sensitive to only one component of the velocity (the one parallel to the average flow). The gap between the disks and the wall of the cylinder is a fraction of a millimeter, so that the flow can be considered as closed. The separation between the disks is 13 cm, thus the aspect ratio of the cell is 0.65. The whole system is enclosed in a temperature regulated (~ 5 K) flask filled with He gas. The cryostat is of the superinsulation kind, with a He reservoir of 80 l.

The delicate point of the experiment is the measurement. We measure the streamwise component of the velocity at one point by "hot wire anemometry." The probe is made from a 7 μm thick carbon fiber [8] whose resistivity behaves with temperature similarly to an Allen Bradley resistance (i.e., the resistivity increases at low temperature); the temperature coefficient $1/R(dR/dT)$ is 0.05 K^{-1}, at 5 K which is a factor of 10 smaller than a typical Allen Bradley. The fiber is stretched across a rectangular frame (6 mm$\times$12 mm) made from 250 μm thick insulated steel wire, and glued to the frame with silver epoxy (to make the electrical contacts) and a droplet of stycast epoxy (for mechanical strength). An evaporation of a good conductor (200 Å of Cr followed by 4000 Å of Au) is then performed on the fiber everywhere except on a spot at the center, which is masked by means of another fiber stretched perpendicularly to the first (this mask is removed in the end). We thus realize a detector that is a cylinder 7 μm in diameter and, depending on the mask size, from 7–25 μm long, the support being 3 mm away from each side. The resistance is typically several hundred Ω at 5 K.

We mounted five such probes at different positions in the cell (marked $A-D$ and F in Fig. 1), the length of the sensitive part being 7 μm for B and C, μm for A, D, and 12 μm for F; the frames A and B were mounted on 1 mm thick steel needles jutting out from the side of the cell, whereas C, D, and F were mounted on a pair of 125 μm thick steel wires stretched across the cell (a similar technique was used, for instance, in Ref. [9]). Both methods gave satisfactory results from the point of view of mechanical stability; at high Re we observe however a series of peaks in the spectrum at high frequencies, which we associate with the von Karman wake created by the detector (the Reynolds number on the detector size varies from about 1 at low densities to about 100 at high densities). Since these peaks are beyond the useful frequency range of the signal, they do not disturb the measurement and we filtered them out. Most of the measurements presented here were obtained with probe B, which is 3.5 cm away from the wall and 2 cm away from the upper disk. This position was chosen in order to have a large mean flow (in the direction of the disk rotation) and at the same time be reasonably far from the walls. The probe is operated at constant temperature (~ 20 K) by homemade electronics. The signal over noise ratio of the system is 80 dB in the best cases (high densities) and 50 dB in the worst (low densities); the bandwidth is about 50 kHz, limited by the speed of the amplifier. The calibration curves, which we obtain by rotating the disks in the same sense, thus creating a rigid body rotation of the whole fluid, are well represented by "King's law" [10], and have been taken into account all the measurements discussed here. The data are digitized by a 16 bit converter controlled by a digital signal processing (DSP) card. A typical sampling rate is 125 kHz, for a typical acquisition time of 5 min.

We also have a global measurement of momentum flux, namely the average torque on the upper disk [11].

In this paper, we define the Reynolds number by the expression

$$\mathrm{Re}=\frac{\Omega R^2}{\nu},$$

where Ω is the angular velocity of the disks, R is the radius, and ν the kinematic viscosity. Some measurements of the statistics at a fixed Re (which were obtained in a similar system, three times smaller in size) have already been described elsewhere [6]; here we concentrate on the Re dependence of the dissipation and related quantities.

III. THE LARGE SCALE STRUCTURE OF THE FLOW

The structure of the mean flow was characterized in a previous work [12], using a similar setup, with the same aspect ratio, and the same number of blades, but with water as the working fluid; the methods used for characterizing the flow were visualization and laser Doppler velocimetry. These studies show that the flow is essentially a mixing layer developing in an axisymmetric geometry. In particular, the velocity profile, plotted along the rotation axis, can be well fitted by a hyperbolic tangential function, like in ordinary mixing layers. The mixing layer may be axisymmetric, or exhibit angular corrugations, usually associated to an azimuthal wave number $m=4$. This pattern may also rotate as a whole, at a velocity much smaller than that of the disks. There is evidence that, for the same external conditions, several states, of slightly different spatial structures, are accessible. For the helium experiment, we do not visualize, but, indeed, it is possible to extract complementary information on the large scale flow from the direct time recording; we thus calculate the energy spectrum $E(f)$ and we transform frequencies into wave numbers k using Taylor's hypothesis; the corresponding relation reads $k=2\pi f/\langle u\rangle$ (where u is the velocity and the bracket denotes time averaging). We find that the average velocity $U=\langle u\rangle$ is, at all Reynolds numbers, 85% of $2\pi R_b f_d$, where f_d is the rotation frequency of the disk and R_b the radial position of the probe. Thus expressing the spectrum in wave numbers amounts to measuring time and lengthscales in units of the rotation frequency of the disks and the size of

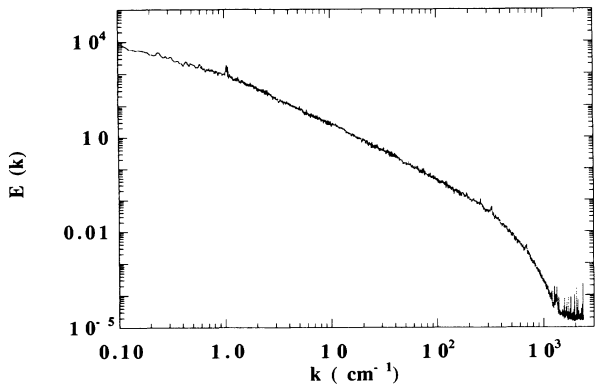

FIG. 2. Power density spectrum of the velocity fluctuation, at 908 mbar, and with a rotation frequency of 20 Hz. The corresponding value of R_λ is 1900. A power law, with an exponent of about -1.72, is apparent over two decades of variation of the wave number.

the box, which are the physical units for this system.

Figure 2 shows an energy spectrum $E(k)$ in the spectral domain, for $\mathrm{Re}\approx 1.2\times 10^6$ (see below for the definition), obtained on probe B; at this high Re, the range of wave numbers where a power law is observed covers more than two decades. The dissipative part of the spectrum is well resolved. The peak at $k\approx 1$ cm^{-1} corresponds to the passage of the six blades; this is the scale at which energy is injected, and from there starts the power law behavior (see also Ref. [13]).

From the spectrum, we can determine several quantities that characterize the large scale structure of the flow: these are the integral scale Λ (defined by $\Lambda=E(0)[\int_0^\infty E(k)dk]^{-1}$) and the longitudinal fluctuation rate u_{rms}/U (here, u_{rms} is the root mean square of the velocity fluctuation—further simply denoted by u'). We plot these two quantities, in Fig. 3, against the Reynolds number Re. There is significant scatter; we have not precisely identified its origin, but it is reasonable to relate it to the fact that on large scales, states of slightly distinct spatial structures are accessible. It nevertheless appears that, within $\pm 25\%$ uncertainty, both quantities are independent of the Reynolds number. The mean value of Λ, which is 4.5 cm, is a fraction of the size of the system. The relatively large fluctuation rate (35%) is consistent with typical values found in mixing layers [14]; the resulting inaccuracies in the application of Taylor's hypothesis will be discussed later. Concerning the large scale structure of the flow, it thus appears that it is independent of the Reynolds number; one could say that our flow belongs to the general class of confined systems, for which the large scale structure is imposed by the boundaries.

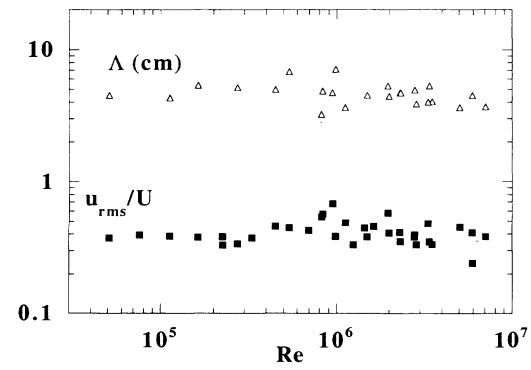

FIG. 3. Evolution with the Reynolds number of the integral scale Λ and the fluctuation rate u_{rms}/U.

IV. MEASUREMENT OF THE DISSIPATION USING THIRD-ORDER STRUCTURE FUNCTIONS

Figure 4(a) shows a typical evolution of the inverse of the longitudinal third-order structure function, defined by

$$F_3(r)=\langle [u(t)-u(t+r/U)]^3\rangle$$

as a function of the separation distance r. In the above expression, $u(t)$ is the local velocity measured by the hot wire, the brackets denote time averaging, and we have applied Taylor's hypothesis to convert time into distance. Figure 4 defines a domain where the structure function is approximately linear in r, in agreement with the von-Karman–Howarth–Kolmogorov relation [15]. A more accurate inspection of the linear regime can be made by plotting the ratio $-F_3(r)/r$, as a function of r, on semi-

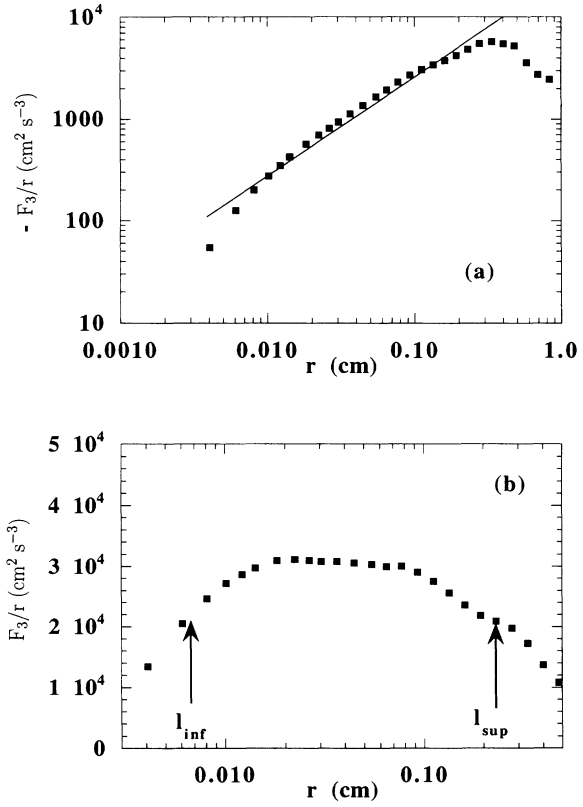

FIG. 4. Third-order structure function $-F_3(r)$ for $R_\lambda\approx 1900$; (a) direct plot on logarithmic scales; (b) plot of the ratio $-F_3/r$ on semilogarithmic scales.

logarithmic scales [Fig. 4(b)]; a plateau can be defined, throughout a range extending over almost one decade in scale. The evidence for the existence of a plateau is generally not as clear as in Fig. 4; one usually has weakly, but significantly rounded plateaus. To investigate the limits where such a plateau can be defined, we introduce two lengths l_{inf} and l_{sup}, arbitrarily defined as the values for which the ratio $-F_3(r)/r$ is equal to 70% of its maximum value. The evolution of these two scales with the Reynolds number is shown in Fig. 5. There is significant scatter in the data, but one can see several trends: concerning the lower scale, we observe first a decrease and further a saturation at a value comprised between 60–120 μm. The decrease of l_{inf} is related to the fact that, as the Reynolds number increases, the inertial range extends farther into the small scale domain. However, the saturation is unexpected in terms of the Kolmogorov picture. Concerning l_{sup}, the scatter is somewhat large, but, as a general trend, one could say that it slightly decreases with the Reynolds number. A typical value of 4 ± 1 mm, i.e., one order of magnitude smaller than Λ, can be suggested to characterize l_{sup} throughout the whole range of Reynolds numbers investigated. The origin of this new scale is not obvious to discuss, on the basis of single probe measurements. It probably expresses the fact that for scales above l_{sup}, turbulence is anisotropic. The value of 4 mm, as an upper limit for anisotropic scales, is consistent with estimates extracted from a numerical study of Taylor-Green vortex [16]. The fact that this value is roughly independent of the Reynolds number differs from observations performed in open flows; this may reflect the fact that we work in a confined geometry, where the large scale flow structure is fixed, while in open systems, even the large scales are generated by the dynamics of the flow itself.

Using the linear region of F_3 we can estimate the dissipation per unit mass ε according to the von-Karman–Howarth–Kolmogorov relation, in the form

$$F_3(r) = -\tfrac{4}{5}\varepsilon r \ . \tag{1}$$

We have checked that the viscous term $v dF_2/dr$ is negligible in all cases. From ε, one can determine several quantities, such as the Kolmogorov scale η, the Taylor scale λ, and the microscale Reynolds number R_λ, defined by

$$\eta = \left[\frac{\nu^3}{\varepsilon}\right]^{1/4}, \quad \lambda = \left[\frac{15\nu u'^2}{\varepsilon}\right]^{1/2}$$

and

$$R_\lambda = \frac{u'\lambda}{\nu} \ .$$

The corresponding results are shown in Fig. 6; the accuracy of the data for values of the Reynolds number below 10^5 is questionable, since the extension of the domain where a power law can be defined is small. Fig-

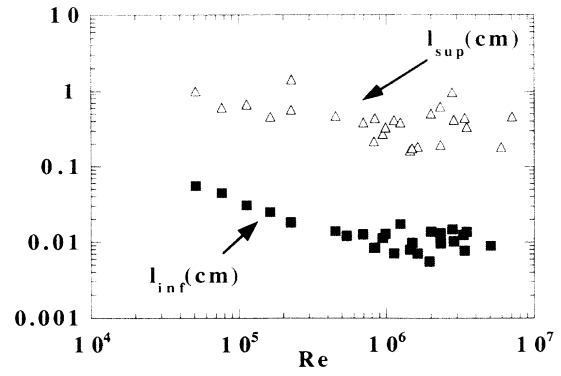

FIG. 5. Evolution with the Reynolds number of l_{inf} and l_{sup}.

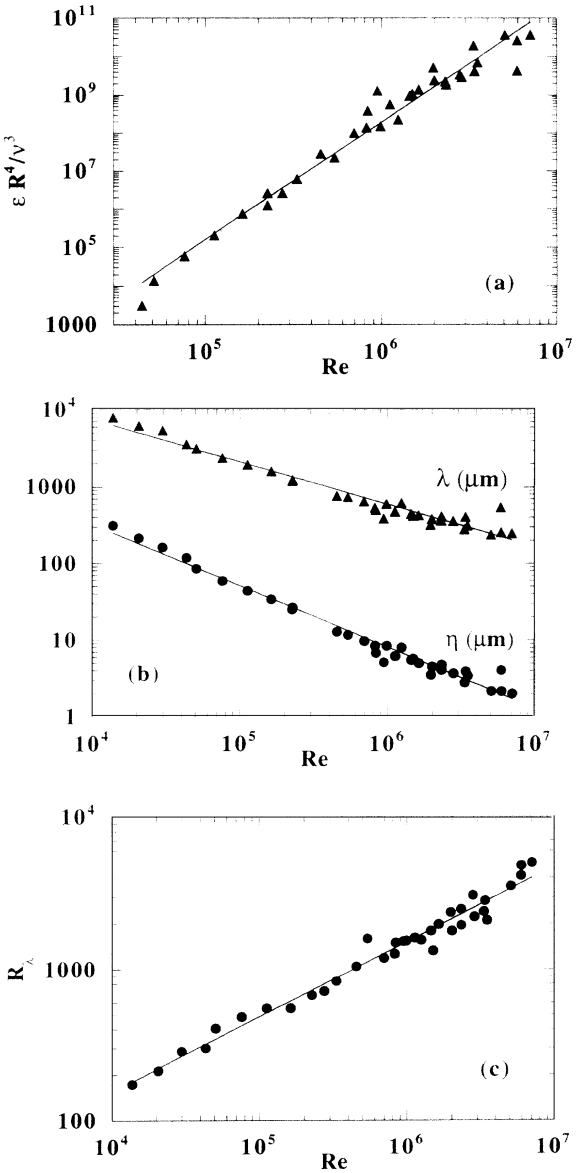

FIG. 6. Reynolds number dependence of (a) dissipation ε, (b) Taylor and Kolmogorov scales, (c) microscale Reynolds number R_λ. For this plot, the dissipation was determined using the third-order structure function.

ure 6 shows the existence of power laws extending over more than two decades in Reynolds number. The corresponding forms are

$$\frac{\varepsilon R^4}{\nu^3}=0.013\mathrm{Re}^{3.06\pm0.1},\quad \frac{\eta}{R}=30\mathrm{Re}^{-0.75\pm0.03},$$

$$\frac{\lambda}{R}=4.9\mathrm{Re}^{-0.49\pm0.03},\quad R_\lambda=1.57\mathrm{Re}^{0.5\pm0.03}.$$

Using the third-order structure function one thus finds values of the exponents in good agreement with the classical estimates, which are three for the dissipation, $-\frac{3}{4}$ for the Kolmogorov scale, $-\frac{1}{2}$ for the Taylor scale and $\frac{1}{2}$ for the Taylor scale Reynolds number. The above relations thus indicate that the form of the "inertial estimate" for the dissipation reads

$$\varepsilon\approx0.013\frac{U^3}{R},$$

or equivalently

$$\varepsilon\approx0.7\frac{u'^3}{\Lambda},$$

which is consistent with measurements performed at smaller values of Re [4].

V. MEASUREMENT OF THE DISSIPATION USING THE SPECTRUM

Here we compute the dissipation ε per unit mass according to [17,2]

$$\varepsilon=15\nu\int_0^\infty dk\, k^2E(k). \tag{2}$$

Figure 7 shows, in the time domain, a typical dissipation spectrum $f^2E(f)$, from which (2) is computed. Again we determine from ε the Taylor scale λ, the corresponding Reynolds number R_λ and the Kolmogorov scale η. Figure 8 shows the plot for R_λ. Fitting with power laws, we find the following exponents:

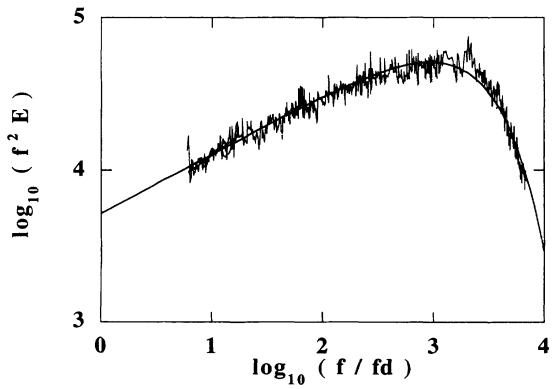

FIG. 7. Dissipation spectrum $f^2E(f)$ with the fit, for $\mathrm{Re}=3.5\times10^6$, $f_d=4$ Hz.

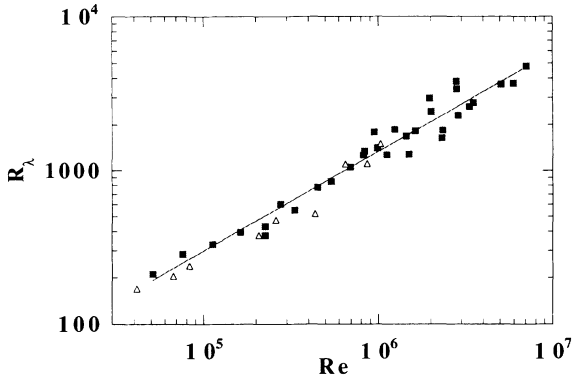

FIG. 8. Log-log plot of R_λ vs Re; the black triangles represent the present experiment, and the white ones a smaller system ($R=3$ cm) with the same aspect ratio [6]; the fit has a slope of 0.65. For this plot, the dissipation was determined using the spectrum.

$$R_\lambda\sim\mathrm{Re}^{0.65\pm0.05},$$

$$\frac{\eta}{R}\sim\mathrm{Re}^{-0.70\pm0.03},$$

$$\varepsilon\sim\frac{U^3}{R}\mathrm{Re}^{-0.30\pm0.10},$$

that is, with this method we observe deviations from the classical scaling.

These exponents are not independent. It is easy to see from the definitions given before that if

$$\varepsilon\sim\frac{U^3}{R}\mathrm{Re}^{\alpha}$$

then

$$\eta\sim R\,\mathrm{Re}^{(-\alpha-3)/4}$$

and

$$R_\lambda\sim\mathrm{Re}^{(1-\alpha)/2}.$$

These measurements thus give $\alpha=-0.3\pm0.1$, while the measurements obtained from the structure function give the Kolmogorov scaling $\alpha=0$.

We now characterize the energy and dissipation spectra more in detail. To this end, it is useful to have a good fit, and we find that the form

$$E(k)\propto k^{-\gamma}/(e^{k/k_0}-1)$$

(which behaves as $k^{-\gamma-1}$ for $k\ll k_0$ and as $k^{-\gamma}e^{-k/k_0}$ for $k\gg k_0$) fits all our spectra reasonably well (see Fig. 7, which shows a typical fit for the dissipation spectrum in the time domain). The cutoff k_0 is related to the Kolmogorov scale η, and we find for k_0 the same scaling exponent, $k_0R\sim\mathrm{Re}^{0.65}$. Using the fit we determine the position k_m of the maximum of the dissipation spectrum (Fig. 7); let us call the corresponding lengthscale $\lambda_m=2\pi/k_m$; we find (Fig. 9)

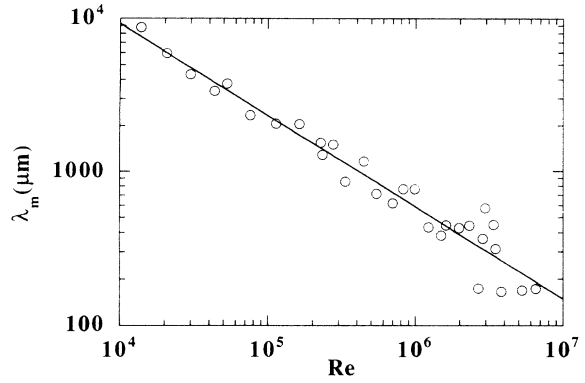

FIG. 9. The position of the maximum in the dissipation spectrum, λ_m (in μm) vs Re; the fit has a slope of -0.60.

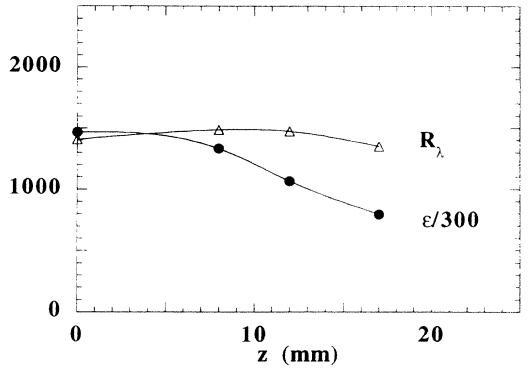

FIG. 11. Spatial evolution of the dissipation and the microscale Reynolds number, measured in the smaller device [6].

$$\lambda_m \sim R\ \mathrm{Re}^{-0.60}\ ,$$

that is, the scale at which the maximum dissipation occurs scales differently from the Kolmogorov scale η. This is related to the fact that the slope of the spectrum (exponent γ) keeps changing; in Fig. 10 we show the evolution of $-(\gamma+1)$, which is the slope of the energy spectrum in the inertial range; it decreases for increasing Re. Consequently the dissipation spectrum $k^2E(k)$ becomes more and more flat (in the inertial range) as Re is increased; the maximum broadens, and shifts to *small* wave numbers when renormalized with the cutoff k_0.

If we extract the exponent of the spectrum by simply fitting a straight line to the "straight" (inertial range) portion we find a similar evolution, but the actual values are somewhat smaller, being comprised between -1.60 and -1.80; this difference is due to the exponential term in the fit. We thus agree with previous experiments in finding slopes of $-5/3$ and smaller, but we show additionally a systematic evolution towards smaller exponents as Re is increased.

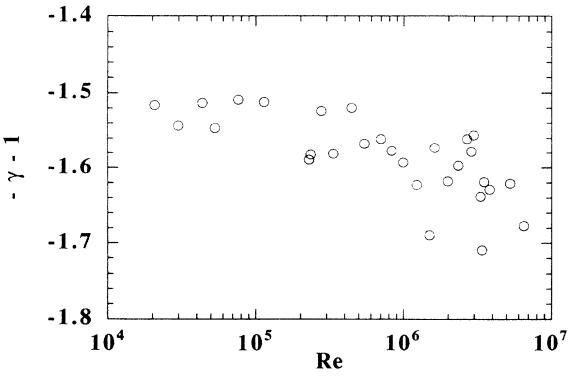

FIG. 10. Semilogarithmic plot of the slope of the energy spectrum (exponent $-\gamma-1$) vs Re.

VI. DEPENDENCE WITH THE POSITION OF THE PROBE

An interesting issue is the spatial dependence of the above characteristics of turbulence in our system. To study that, we used a smaller device [10], and displaced an anemometer mounted on a step by step motor. The displacement was performed along a line parallel to the rotation axis, 2 cm apart (in this setup, the radius was 3 cm). Figure 11 shows the evolution of the dissipation ε, and the microscale Reynolds number R_λ, measured by using the third-order structure function. On the figure, $z=0$ represents the midplane and $z=25$ mm the lower plane of the blades. One can see that the dissipation is maximum at the midplane and decreases as we approach the disk; this spatial evolution is consistent with known characteristics of the mixing layer [14]. We find that the spatial variations of R_λ are much smaller; this is due to the fact that both u' and ε increase as we approach the midplane; thus, R_λ can be taken as a constant throughout the layer, and therefore, it provides a useful parameter for characterizing the whole system.

VII. DISCUSSION ON THE TAYLOR HYPOTHESIS

The high fluctuation rate (35%) may introduce uncertainties in the application of the Taylor hypothesis. This is a point that certainly merits attention and experiments are in preparation to estimate the effect of large fluctuations. Several correction schemes have been elaborated in the past [18], and more recently [19], to take this effect into account. According to Ref. [18], the corrected value ε′ of the dissipation reads

$$\varepsilon' = \frac{\varepsilon}{1+\dfrac{u'^2}{U^2}+2\dfrac{v^2}{U^2}+2\dfrac{w^2}{U^2}} \tag{3}$$

in which v and w are the transverse components of the turbulent fluctuations [see formula (36) of Ref. [18]]. In a mixing layer, close to the edges, such quantities amount to typically 60% the longitudinal component u' [14]; thus the above formula shows that we overestimate the

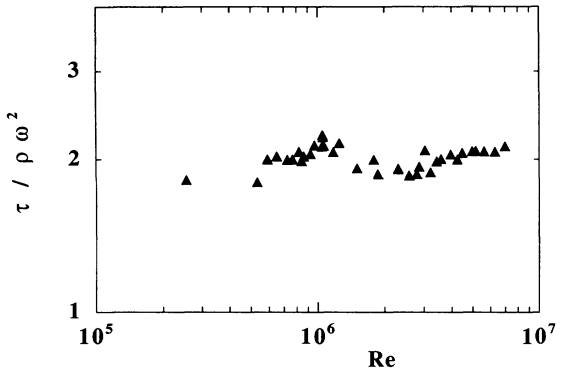

FIG. 12. Dimensionless torque $\Gamma/\rho\Omega^2$ (arbitrary units) vs Re. A power-law fit gives an exponent of zero within the errors.

dissipation by a factor of 30% while R_λ and η are underestimated by 15% and 8%, respectively. Another consequence of the above formula is that, if the large scale structure is fixed, the correction is independant of the Reynolds number. In our case, as previously mentioned, we have a strong indication that this is the case, since the longitudinal fluctuation rate, the integral scale, and (according to Ref. [12]) the mean flow are independent of the Reynolds number. Therefore, such corrections should not change the values of the exponents that we find and more generally the form of the functional dependence of the dissipation with the Reynolds number.

VIII. EVOLUTION OF THE TORQUE WITH THE REYNOLDS NUMBER

We measure the torque Γ exerted by the fluid on the lower face of the upper disk. At low densities we are limited by the sensitivity of the method, so that we have to restrict ourselves to the range $5\times10^5 \le \mathrm{Re} \le 10^7$. Also, we present only relative measurements, since the absolute value has not been calibrated. Figure 12 shows that the (dimensionless) measured torque $\Gamma/\rho\Omega^2$ (Γ is the torque, ρ the density, and Ω the angular velocity of the disk) is independent of ν. The total power $P=2\Gamma\Omega$ is then also independent of ν. Thus the "inviscid estimate" holds for the global dissipation per unit mass P/M (M is the total mass of the He). We note that P (estimated by using the value of the electric power provided to the motors, subtracting the contribution in the corotating mode) is found much larger than the value of ϵ integrated over the bulk volume. Therefore, most of the power is dissipated in regions outside the bulk. These can be located either between the blades or in boundary layers close to the walls. In any case, the global dissipation per unit mass P/M and the bulk value ϵ are quite distinct quantities.

IX. DISCUSSION AND CONCLUSION

We first compare the two methods of determination of the dissipation in the bulk (third-order structure function and the spectrum). The problem that is raised by our measurements is that the exponents found by the two methods are not the same. If we compare Figs. 6 and 8, we can fairly say that the two measurements are consistent for Reynolds numbers above 5×10^5. For lower values, discrepancies are clearly visible; we can have a factor of 3 between the two estimates of R_λ (or ϵ) at the smallest Re. Both methods are based on the assumption of statistical isotropy and homogeneity of the small scales of the flow. If this condition is partially violated, it is not immediately clear which of the two determinations of ϵ will be affected most.

Concerning the structure function method, we remark that the expected scaling of the function with r is of modest quality. It has been argued [20] that edge effects are responsible for the degradation of these power laws, but there is no evidence that this is indeed the case. In any case, for $\mathrm{Re}<10^5$ the limited extent of the inertial domain makes this determination of ϵ problematic.

The method that uses the spectrum does not suffer from the limitations resulting from a small inertial range at low Re; however, if the dissipative scales are anisotropic at low Re (due to the proximity, in wave-number space, of the forcing) the coefficient 15 in (2) (which comes from the fact that we measure a one-dimensional spectrum) may actually take a different value, and may indeed depend on the Reynolds number, for low enough Re.

In the present state of affairs, it is difficult to conclude which of the two methods gives a better determination of ϵ. One of us (G.Z.) gives credit to the measurements of the dissipation by the spectral method, and tends to conclude to the existence of deviations from the classical scaling. Two of the authors (P.T. and H. W.) are inclined to think that a more direct measurement of the anisotropy is needed for drawing a definite conclusion. We shall not elaborate here on the consequences that a viscosity dependent dissipation would have for our understanding of turbulence: they are obviously far reaching.

ACKNOWLEDGMENTS

This work was rendered possible by the help of many people. M. Usseglio and G. Jouve did the critical solderings, J. C. Sutra the mechanical parts, and the ENS central shop the cryogenic ones. The thesis of Xiao Zhong Wu [9] was invaluable in designing the experiment. R. Hildebrand and A. Libchaber provided us with IR bolometers with which the first measurements were started. O. Cardoso wrote the data acquisition program. We are indebted to the students of the Radioastronomie group at ENS, in particular H. Charabani, for allowing, and instructing us on, the use of the evaporator. Y. Couder, O. Cadot, S. Douady, E. Siggia, M. E. Brachet, B. Perrin, C. Guthman, F. Heslot, S. Balibar, O. Cardoso, B. Castaing, and A. Libchaber helped at various stages through ideas and discussions. This work was supported by CNRS, the EC, and DRET Contract No. 92/114.

[1] See for instance, A. S. Monin and A. M. Yaglom, *Statistical Fluid Mechanics* (MIT, Cambridge, MA, 1975), and references therein.
[2] H. Tennekes and J. L. Lumley, *A First Course in Turbulence* (MIT, Cambridge, MA, 1989).
[3] A. N. Kolmogorov, C. R. Acad. Sci. USSR **30**, 301 (1941).
[4] K. A. Sreenivasan, Phys. Fluids **27** (5), 1048 (1984).
[5] F. Heslot, B. Castaing, and A. Libchaber, Phys. Rev. A **36**, 5870 (1987).
[6] J. Maurer, P. Tabeling, and G. Zocchi, Europhys. Lett. **26**, 1 (1994); **26**, 31 (1994).
[7] S. Douady, Y. Couder, and M. E. Brachet, Phys. Rev. Lett. **67**, 983 (1991).
[8] This idea, and the fiber itself, we owe to the courtesy of B. Chabaud and B. Castaing.
[9] X. Z. Wu, Ph.D. thesis, University of Chicago, 1991.
[10] J. O. Hinze, *Turbulence* (McGraw-Hill, New York, 1987).
[11] The measurement technique, which relies on strain gauges, was inspired by the turbulent Taylor-Couette flow experiment of H. Swinney's group in Texas.
[12] O. Cadot (private communication); see also [7].
[13] M. Sano, X. Z. Wu, and A. Libchaber, Phys. Rev. A **40**, 6421 (1989).
[14] A. A. Townsend, *The Structure of Turbulent Shear Flow* (Cambridge University Press, Cambridge, 1980).
[15] T. von Karman and L. Howarth, Proc. R. Soc. London, Ser. **164**, 192 (1938).
[16] J. Jimenez, A. Wray, P. Saffman, and R. Rogallo, J. Fluid Mech. **255**, 65 (1993).
[17] G. I. Taylor, Proc. R. Soc. London, Ser. A **164**, 476 (1938).
[18] See, F. H. Champagne, J. Fluid Mech. **86**, 67 (1978), and references therein.
[19] J. F. Pinton and R. Labbé, J. Phys. II. (to be published).
[20] M. Nelkin, Phys. Fluids **24**, 556 (1981).